Temperature and pressure study of Brillouin transverse modes in the organic glass-forming liquid orthoterphenyl

C. Dreyfus,[1,*] A. Aouadi,[2] J. Gapinski,[3] M. Matos-Lopes,[4] W. Steffen,[2] A. Patkowski,[3] and R. M. Pick[1]
[1]*PMC and UFR 25, Case Postale 86, UPMC, 4 Place Jussieu, 75005 Paris, France*
[2]*Max Planck Institute for Polymer Research, Ackermannweg 10, 55128 Mainz, Germany*
[3]*Institute of Physics, Adam Mickiewicz University, Umultowska 85, 61-614 Poznan, Poland*
[4]*Departamento de Quimica et Bioquimica, Universidade de Lisboa, 1749-016 Lisboa, Portugal*
(Received 26 December 2002; published 15 July 2003)

Transverse Brillouin spectra of orthoterphenyl are measured in the (250–305 K; 0.1–100 MPa) temperature-pressure range, which corresponds to the supercooled phase of this organic glass former. We show that the analysis of these spectra combined with an extrapolation of the reorientation times under pressure leads to an estimate of the static shear viscosity in a pressure range whose validity extends beyond the range of the Brillouin measurements. The relative contributions of temperature and of density to the change of this reorientation time measured along an isobar are extracted from our results in a large temperature range extending from the liquid to the low temperature supercooled state. They appear to be always of the same order of magnitude. It is also shown that in the range of the experiment, the orientational time is depending on a unique parameter built on temperature and density.

DOI: 10.1103/PhysRevE.68.011204 PACS number(s): 66.20.+d, 78.35.+c, 64.70.Pf

I. INTRODUCTION

A well-known characteristic of the liquid to glass transition at ambient pressure is the tremendous increase in shear viscosity as temperature decreases. At the same time, some of the motions inside the fluid slow down in the same proportion. This phenomenon is linked to the structural relaxation, the increase in shear viscosity being actually a signature of it. Similar increases in viscosity and structural relaxation time are observed when pressure is increased at constant temperature. Actually the relevant thermodynamical parameters are temperature and density, the latter increasing when pressure increases and increasing also when temperature decreases. As both parameters can drive the liquid-glass transition, only experiments in which temperature and pressure are changed can allow to disentangle both effects and to determine their relative importance, which is of great theoretical interest [1]. While the description of the structural relaxation at variable temperature and constant ambient pressure is now well documented [2], the amount of data obtained at variable temperature and pressure is still rather sparse, because of experimental difficulties, so that only few studies are available.

Among the numerous glass formers, those belonging to the ''fragile'' type [3], i.e., the thermal variation of their viscosity is strongly non-Arrhenius, are of special interest. So far, this behavior is still not well understood and some of the theories of the liquid-glass transition are expected to be particularly effective in its description [2].

Orthoterphenyl (OTP) belongs to this family and is one of the most studied glass-forming liquids [4]. At ambient pressure, several dielectric, neutron, and light scattering studies have been published [4–8]. OTP under pressure is also quite well documented: shifts of the liquid-glass transition temperature with pressure [9], determination of the equation of state [10], dielectric measurements [11], dynamic light scattering [12], neutron diffusion [13], specific heat spectroscopy [14], and viscosity [15] measurements have been done.

Transverse diffusive modes always exist in liquids [16]. In glass-forming liquids formed of anisotropic molecules, a striking feature is the observation of propagative transverse waves in the fluid phase provided the frequency of the probe is high enough [17]. The progressive transformation of these transverse modes from a diffusive to a propagative behavior upon cooling has been the object of numerous experimental and theoretical studies [18–20]. Very recently, a complete theory of the phenomenon was given [21,22] in terms of a set of coupled equations of motions for the mass density and the mean local orientation of the molecules, which take into account a rotation-translation coupling. These equations can be rigorously derived [22] taking into account retarded effects to which correspond specific memory functions. An interesting aspect of this theory is that it allows one to derive from light scattering experiments, performed at temperatures at which propagative modes are detected, the value of the static shear viscosity that should be measured at the same temperature by classical viscosimetry, and this prediction has been verified already in a few instances [21,23].

In this paper, we analyze the transverse propagative modes in OTP measured under variable temperature and pressure. We discuss in detail different options of the analysis and their impact on the results and more particularly on the relaxation times and viscosity. Although this discussion may appear somewhat intricate, it leads to a simple assumption on relaxation times measured at ambient pressure which is then validated when extended to high pressure. Taking advantage of the wealth of data already existing for this molecular glass former and of the results of the analysis, we show that the orientational relaxation time is a function of a unique parameter built as a simple power law of temperature

*Author to whom correspondence should be addressed.

and density and we determine the relative importance of the parameters' density and temperature in the thermal variation of the structural relaxation time in a large range of temperatures.

In the following section, we summarize the main theoretical results concerning the detection of the transverse modes in a light scattering experiment. In Sec. III, we describe the experimental setup and the results obtained by us. In the following one, results of the analysis of the ambient pressure experiments are discussed. In Sec. V, we propose an expression for the rotational relaxation time, valid in the temperature-pressure domain, and we show that this expression is consistent with the high-pressure light scattering and viscosity measurements. Finally, we discuss the relative importance of temperature versus density effects in the glass-forming liquid OTP.

II. THEORETICAL BACKGROUND

A. Transverse modes in supercooled liquids of anisotropic molecules

In liquids formed of anisotropic molecules, the depolarized light scattering (DLS) spectrum contains a central peak corresponding to the reorientational dynamics of these molecules, which is detected through the corresponding change in the anisotropic polarizability tensor [24]. Due to the very small wavelength of the scattering wave vector q, this dynamics can be considered in its $q=0$ limit. As is well known since the beginning of the 1970s [17,18], transverses modes characterized by their wave vector can also be detected by this mechanism. The complete theory [21] involves a set of coupled hydrodynamic equations that considers both the motions of the centres of mass of the molecules and their mean local orientation. These equations contain a rotation-translation coupling between those two variables, which is characterized by its strength Λ and a memory function describing the retarded aspect of this coupling. This theory generalizes earlier works, in particular those of Quentrec [19] and Wang [20].

In the frequency range of interest, for the depolarized light scattering experiments we shall analyze, the intensity can be written [21] as

$$I_{\mathrm{aniso}}(\omega)\propto\frac{1}{\omega}\mathrm{Im}\left[R(\omega)+\cos^2\theta/2\,\frac{\Lambda q^2\rho_m^{-1}R^2(\omega)}{\omega^2-\omega\rho_m^{-1}q^2\eta_T(\omega)}\right], \tag{1}$$

where ρ_m is the mass density, θ is the scattering angle, and q the wave vector; $\eta_T(\omega)$ is the "total shear" viscosity given by

$$\omega\eta_T(\omega)=\omega\eta_S(\omega)-\Lambda R^2(\omega)/[1-R(\omega)], \tag{2}$$

where $\eta_S(\omega)$ is the frequency-dependent shear viscosity without translation-rotation coupling (i.e., bare viscosities related only to the motion of the centres of mass). The first term of Eq. (1), proportional to $R(\omega)$, represents the low-frequency part of the rotational dynamics while the second describes the intensity due to the transverse mode. This second term is proportional to Λ, the rotation-translation coupling strength. The numerical study of that term shows that its spectral shape is mostly determined by the frequency dependence of $\eta_T(\omega)$, the numerator representing only the coupling of the mode to the light scattering mechanism. The appearance of $R^2(\omega)$ in the denominator is the result of an approximation in which one admits that the memory function characterizing the rotation-translation mechanism is very similar, at low frequency, to that describing the rotational dynamics. Due to the $\cos^2(\theta/2)$ term in Eq. (1), the transversal modes cannot be detected in backscattering geometry.

The transverse viscosity $\eta_T(\omega)$ given in Eq. (2) is the sum of the shear viscosity $\eta_S(\omega)$, due to the centres of mass motion, and of a second term due to the coupling of the centres of mass motion to the orientational dynamics. This second term depends on the coefficient Λ and on an expression in $R(\omega)$ representing the contribution of the orientation coupling to $\eta_T(\omega)$. Its influence will be minimal as long as Λ is a small quantity.

Let us notice the following.

(i) The denominator of the second term of Eq. (1) characterizes the dynamics of the transverse modes at frequency ω. With our definition of the Fourier-Laplace transform [25],

$$\lim_{\omega\to 0}\eta_T(\omega)=i\eta_S, \tag{3}$$

where η_S is the static shear viscosity at the same temperature. As $R(\omega)$ is the susceptibility associated with the rotational dynamics (see Ref. [1]),

$$\lim_{\omega\to 0}\left[\frac{1}{\omega}R^2(\omega)\right]=0. \tag{4}$$

This yields, at every temperature, the exact relationship

$$\eta_S=(-i)\lim_{\omega\to 0}\eta_S(\omega). \tag{5}$$

(ii) Conversely, for large enough wave vectors, the transverse modes are always propagative and weakly damped in this hydrodynamics approach [21,22]. The corresponding transverse velocity is given by

$$v_T=\left[1-\Lambda\frac{R^2(\omega)}{\eta_S(\omega)[1-R(\omega)]}\right]^{1/2}_{\omega\to\infty}\left[\frac{\eta_S(\omega)}{\rho_m}\right]^{1/2}_{\omega\to\infty}$$
$$=r\left[\frac{\eta_S(\omega)}{\rho_m}\right]^{1/2}_{\omega\to\infty}, \tag{6}$$

r is called the reduction factor, and the closer it is to unity the smaller Λ is: a simple reading of the peak of the depolarized spectrum gives a good estimate of $\eta_S(\omega)_{\omega\to\infty}$ as long as Λ is a small quantity (see the Appendix for a discussion of the limits).

B. Frequency dependence of the memory functions

The use of Eq. (1) to analyze depolarized spectra implies the knowledge of the functional form of $\eta_S(\omega)$ and of $R(\omega)$. $R(\omega)/\omega$ is the Laplace transform of the long time part of the orientational dynamics while $\eta_S(\omega)$ is a similar Laplace transform for the memory function coupling the instantaneous stress tensor to the strain rate tensor of the liquid. Assuming for these functions a Debye relaxation mechanism, $\sigma(t)=\sigma_0\exp[-(t/\tau)]$, leads to the well-known Maxwell formulation of viscoelasticity. Actually, in most supercooled liquids, it appears that this formulation oversimplifies the representation of the relaxation process. More realistic representations have to be used for its description. The simplest extension of the Debye relaxation function is the stretched exponential (or Kohlrausch) function $\sigma(t)=\sigma_0\exp[-(t/\tau_K)^{\beta_K}]$, its associated frequency-dependent Fourier Transform [2] $\sigma(\omega)$ being often conveniently approximated by the Cole-Davidson function:

$$\sigma(\omega)=\frac{-i\sigma_0}{\omega\beta_{\mathrm{CD}}}\left[1-\left(\frac{1}{1+i\omega\tau_{\mathrm{CD}}}\right)^{\beta_{\mathrm{CD}}}\right], \tag{7}$$

the parameters β_{CD} and τ_{CD} being related to the parameters of the stretched exponential β_K and τ_K by expressions given in Ref. [26]. Nevertheless, studies performed in the last decade have shown that Eq. (7) is insufficient to describe the higher-frequency results. We have thus to discuss how Eq. (7) has to be used and what has to be added in the high-frequency domain to describe the features there.

In the case of the rotational dynamics, the low-frequency part of $R(\omega)\approx\omega\sigma(\omega)$ has to be written as

$$R(\omega)=R_0\left\{1-\left(\frac{1}{(1+i\omega\tau_R)}\right)^{\beta_{\mathrm{CD}}}\right\}, \tag{8}$$

with $0<R_0<1$, R_0 being the weight of the α relaxation process in the total orientation dynamics. Equation (8) thus leads to an experimental determination of the corresponding β_{CD} and $\tau_R(T)$. This equation does not describe the high-frequency part of $R(\omega)$, which exhibits [27] a minimum in the susceptibility at frequencies higher than the α relaxation process, and then an increase up to the THz region. These two last features have been interpreted within the mode coupling theory (MCT) [2] as the signature of a so-called β-fast process, and, in particular, the increase of $R(\omega)$ has been named the critical decay process. Even if the MCT is applicable, in the best molecular liquid cases, to a temperature domain smaller than the one we shall explore here, we shall keep, for simplicity, this nomenclature in the present paper. In the frequency domain of existence of this critical decay, $R(\omega)$ is expected to behave as ω^a with $0<a<1$, so that it will be necessary to replace Eq. (8) by

$$R(\omega)=R_0\left[\left\{1-\left(\frac{1}{(1+i\omega\tau_R)}\right)^{\beta_{\mathrm{CD}}}\right\}+ig\omega^a\right], \tag{9}$$

following an approximation close to that given in Ref. [28]. In principle, other fast relaxation processes corresponding to the coupling of this dynamics to fast decaying variables could also be introduced. In the range of frequency of interest, this coupling is usually written as $i\omega\gamma_R$ and should be added in Eq. (9).

Though $\eta_S(\omega)$ is a memory function and not a correlation function, the same functional form is expected to hold, which yields

$$\omega\eta_S(\omega)=G_\infty^\alpha\left\{1-\left(\frac{1}{(1+i\omega\tau_s)}\right)^{\beta_{\mathrm{CD}}}\right\}+ig_s\omega^a+i\omega\gamma_s \tag{10}$$

with same values for a and β as in Eq. (9).

Contrary to R^0, G_∞^α is not a number but an elastic shear modulus [see Eq. (6)], which simply needs to be positive. In the Appendix, we show that the functional form, Eq. (10), containing g_s and γ_s, is only valid in the frequency domain of interest for the light scattering spectra, but is appropriate for computing the two limits mentioned in Eqs. (5) and (6). The proper use of these limits yields

$$\eta_S=G_\infty^\alpha\tau\beta_{\mathrm{CD}} \tag{11}$$

and

$$r=[1-\Lambda R_0^2 G_\infty^{-1}(1-R_0)^{-1}]^{1/2}. \tag{12}$$

III. EXPERIMENT

The light scattering spectra at all temperatures and pressures were taken using a 6-pass Tandem Fabry-Perot Interferometer (JRS) and an optical system described in detail elsewhere [29]. The incident beam from an argon-ion laser operating in a single mode at $\lambda=514.5$ nm at a power of about 400 mW and the scattered beam was polarized vertically (V) and horizontally (H) to the scattering plane, respectively, using the Glan and Glan-Thompson polarizers. A narrow band interference filter was used in order to suppress the contributions of higher orders to the DLS spectrum [30].

The high-pressure light scattering cell was described in detail elsewhere [31]. The pressurizing medium was nitrogen. The temperature range of the cell is from -30 to 150 °C and the pressure range is 1–2000 bar. The aperture of the windows of the pressure cell is 2.4°.

The commercially obtained OTP (Merck-Schuchardt, $T_g=244$ K, $T_m=329$ K) was carefully distilled and filtered (0.22-μm Millipore) directly into dust-free cylindrical deactivated Pyrex cells (inside diameter 10 mm) to avoid crystallization as much as possible. Nevertheless, crystallization occurred often during the experiments at high pressure and is the major difficulty in carrying out the measurements.

In order to detect the transverse Brillouin spectra, a 90° VH scattering geometry was used in our ambient and variable pressure experiments. Furthermore, at ambient pressure backscattering VH geometry spectra were also measured. Ambient pressure experiments were performed in a purpose built oven with an aperture of 5°. High-pressure experiments were done for 20, 40, 60, 80, and 100 MPa in 90° VH geometry. Figure 1 shows the thermal variation of the transverse Brillouin lines at ambient pressure and variable temperature. The full lines are fits to the data as described later.

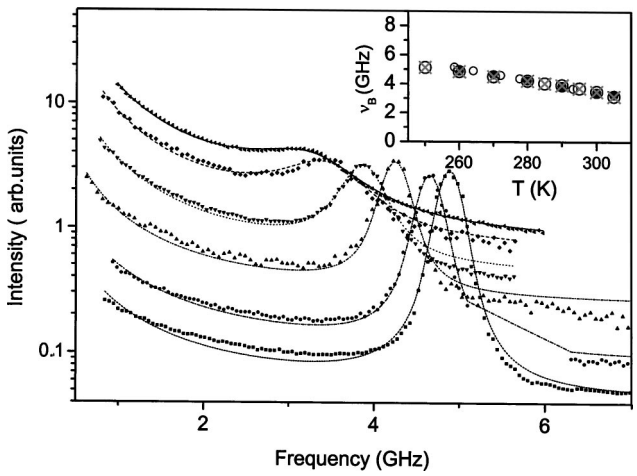

FIG. 1. Transverse mode: Experiments and fit to the data following Eqs. (1), (10), and (11); ambient pressure, variable temperature: (■) 260, (●) 270, (▲) 280, (▼) 290, (♦) 300, (◀) 305 K. Inset: transverse Brillouin frequencies at 90° scattering geometry, this work, (●); Ref. [5], (○); Ref. [6(b)], (⊗).

The Brillouin linewidth decreases and the Brillouin frequency increases with decreasing temperature. As shown in the inset of Fig. 1, the transverse Brillouin frequencies are in very good agreement with results already published [5]. In Fig. 2 and in Fig. 3, respectively, the pressure variation of the transverse Brillouin lines at constant temperature (300 K) and the temperature variation of the transverse Brillouin lines at constant pressure (100 MPa) are shown. As in Fig. 1, lines are fits to the data. To show the relation between the contribution from the rotational and the transversal modes, we matched two spectra taken at 300 K in backscattering and in 90° scattering geometry and show them in Fig. 4. Lines are again fits to the data and are explained in the following section.

IV. ANALYSIS OF THE AMBIENT PRESSURE EXPERIMENTS

The theoretical frame summarized in Sec. II allows us to analyze the transverse modes at ambient pressure, thus to determine in principle at each temperature, the shear relaxation times and shear elastic modulus and compare them to the static shear viscosity values. We shall see that the results lead finally to a suggestion for analyzing the spectra recorded at high pressure where we have much less spectral information.

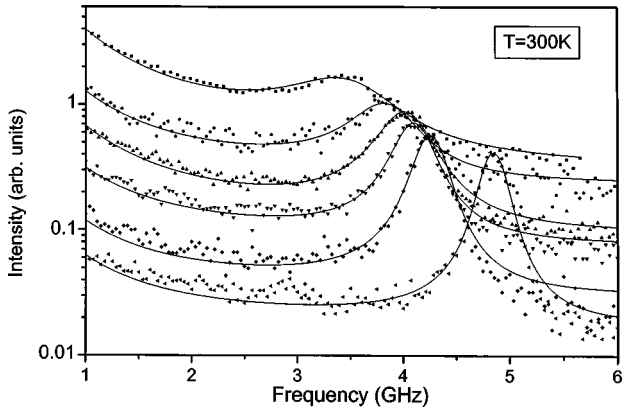

FIG. 2. Transverse mode, Experimental and fit; variable pressure, constant temperature (300 K): (■) ambient, (●) 20, (▲) 40, (▼) 60, (♦) 80, (◀) 100 MPa.

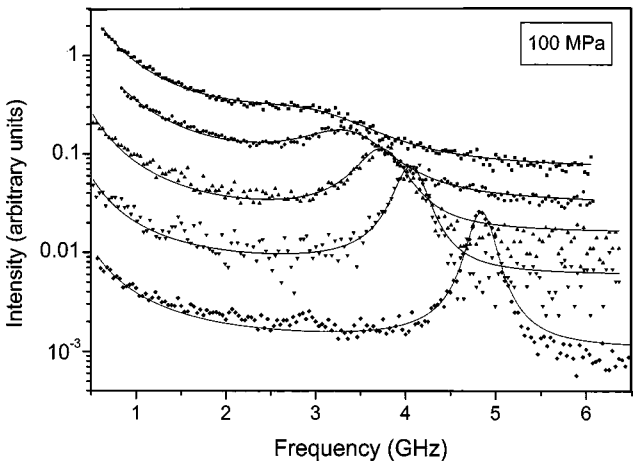

FIG. 3. Transverse mode, Experimental and fit; constant pressure (100 MPa); variable temperature: (■) 340, (●) 330, (▲) 320, (▼) 310, (♦) 300 K.

A. Analysis of the transverse modes

The information contained in the backscattering and in the 90° depolarized spectra in the limited range accessed in our experiments is insufficient to determine all the parameters entering into Eqs. (1), (10), and (11). To circumvent this difficulty, in a first analysis, we use the rotational relaxation time τ_R and the stretching parameter [32] β_{CD} obtained from previously published experiments [6]. We thus simply adjust at each temperature the two parameters a and g to fit the

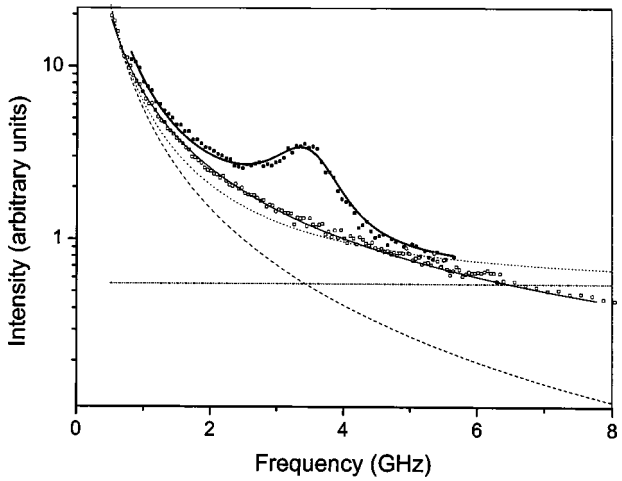

FIG. 4. Transverse mode analysis at 300 K and ambient pressure: (■) 90° depolarized spectra, (——) fit to the 90° depolarized spectra, (– – –) Cole-Davidson (CD) contribution, (–·–·–·–) background contribution, (· · · ·) sum of the CD and background contributions, (□) depolarized backscattering intensity, (——) fit to the depolarized backscattering intensity by Eq. (10).

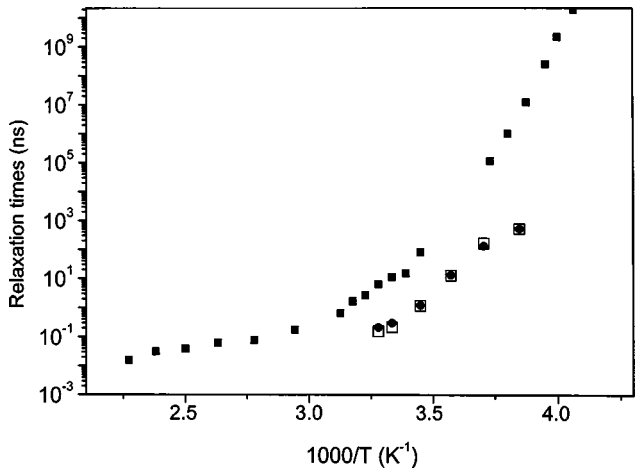

FIG. 5. Relaxation times: rotational time τ_R and shear time τ_s obtained at ambient pressure from Sec. IV: τ_R from Ref. [6], (■); τ_s where $R(\omega)$ is the backscattering spectrum and $\gamma=0.1$ GHz (●); τ_s where $R(\omega)$ is a Cole-Davidson function and $\gamma=0.1$ GHz (□).

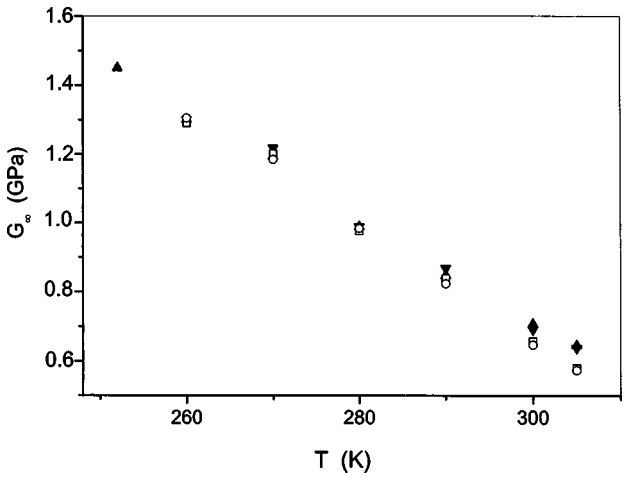

FIG. 6. Shear modulus G_∞^α at ambient pressure: without constraint on τ_s, using the best fit for $R(\omega)$ (Sec. IV A) (▲); without constraint on τ_s, $R(\omega)$ being represented by a Cole-Davidson function (Sec. IV B) (▼); including fast relaxation process for $\tau_R/\tau_s=10$ (□); G_B (○).

experimental data. The experimental backscattering intensity $R(\omega)/\omega$ measured at 300 K and fits to this profile by Eq. (10) are shown in Fig. 4. The fit is good in the whole frequency domain over which we have measured the depolarized backscattering spectrum.

To fit the latter, we have first made the hypothesis, already made explicit in Eqs. (10) and (11), that the stretching coefficients β_{CD} are the same for $R(\omega)$ and $\omega\eta_S(\omega)$. Also, we set g_s to zero and estimated γ_s, assuming it to be temperature independent. Its value was deduced from the value of the intrinsic Brillouin linewidth below the glass transition temperature and was found to be 0.1 GHz [33]. Thus the fitting equation involves four free parameters: R_0, G_∞, τ_s, and Λ. The result of the fit is shown in Fig. 1 together with the experimental data at 90°: the agreement is satisfactory at all temperatures in the frequency range considered. Nevertheless, considering the rather narrow frequency domain of the fit, a question that has to be considered is the validity of the parameters determined in this way.

Shear relaxation times and infinite frequency shear moduli (see the Appendix) are obtained from the fit, which yields the values of the shear viscosity following Eq. (12). These quantities are shown, respectively, in Figs. 5–7. Figure 5 compares over a large thermal range the rotational [6], τ_R, and shear relaxation, τ_s, times. This figure shows that $\tau_s<\tau_R$ whatever the temperature. Both times almost scale by a factor of the order of 30. Although orientational and shear relaxation times have already been found to be different in other glass-forming liquids, this difference was much smaller than that in the present case: a scaling factor $\tau_R/\tau_s=2.43$ was found in $ZnCl_2$ [23] and, in *m*-toluidine [21] at high temperatures, the ratio was $\tau_R/\tau_s=4$.

The infinite frequency shear modulus is shown in Fig. 6. As it has been found previously in *m*-toluidine, its value decreases with increasing temperature, in the present case by more than 50%, for a relative variation of the temperature of ~20%. Comparing it to the apparent shear modulus obtained directly from the frequency of the transverse Brillouin line, one finds that it is only at high temperatures that it differs slightly from the elastic modulus computed directly from the frequency ω_B of the Brillouin transverse modes ($G_B=\rho_m\omega_B^2/q^2$).

Comparison between computed and experimental values of the static shear viscosity is shown in Fig. 7. In the two previous cases already mentioned, both values coincide at least in a limited temperature range. This is not the case here. Though the thermal variations of the calculated and measured static viscosities follow rather similar non-Arrhenius thermal variations, the computed values are smaller than the directly measured ones by more than one order of magnitude, even at the highest temperature, implying that there are additional contributions to the linewidths. Since the high-frequency parts of the relaxation function have not been yet taken into account, this could be the reason for this discrepancy.

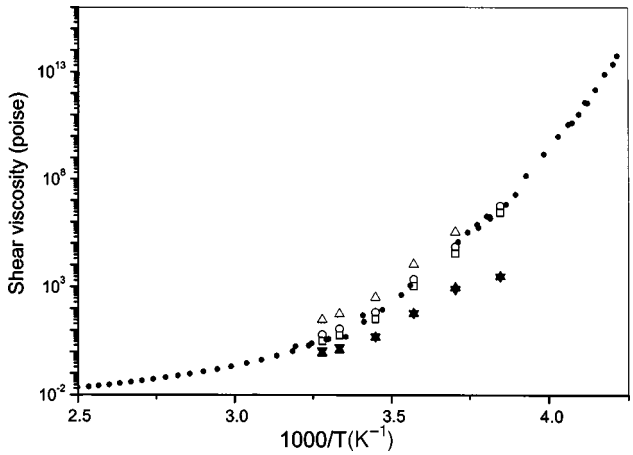

FIG. 7. Static shear viscosity: (●) η_S at ambient pressure [40–43]; fit without critical decay contribution in $\eta_S(\omega)$, (▲), (▼) as in Fig. 6; fit with a critical decay contribution, (□) $\tau_R/\tau_s=10$, (○) $\tau_R/\tau_s=5$, (△) $\tau_R/\tau_s=1$ (cf. Sec. IV C).

Turning now to the value of the reduction coefficient r given by Eq. (12), we find that it varies from 0.97 to 0.995, i.e., r is very close to 1. In other studies, the value was $r=0.95$ for $ZnCl_2$ [23] and r varying from 0.8 to 0.93 for *m*-toluidine [21,34]. Such a r value very close to 1 shows that the coupling between shear and rotation motions is very small in OTP, a fact which can be attributed to the almost globular shape of this molecule. This is in line with recent transient grating results, which show [35] that no appreciable orientation-translation coupling is present in OTP, contrary to what is observed in salol [36] and *m*-toluidine [37]. As a consequence, the weakness of the coupling does not allow to determine the parameters characterizing the coupling with a good accuracy. Therefore, the robustness of the values of the parameters with the options of the fit must be considered.

B. Discussion of the reorientation contribution $R(\omega)$

The reorientation contribution $R(\omega)=\omega I(\omega)$ introduced in the fit described in Sec. IV A was obtained from depolarized backscattering measurements at ambient pressure. Backscattering experiments are not possible under pressure in our experiment because of the small aperture of the high-pressure cell. It is thus important to find out if we can define a function $R(\omega)$ depending on parameters that we can obtain through an easier route and which can be used in the analysis of the transverse modes.

We have tested this possibility by performing a second fit in which $R(\omega)$ is simply approximated by a Cole-Davidson function ($g=0$). The total spectrum $I_T(\omega)$ is given by Eq. (1) plus a background added in order to take care of the high-frequency tail of $R(\omega)$. This amplitude is a free parameter and the parameter of the Cole-Davidson function is taken as previously. This procedure gives reasonable fits of the backscattering depolarized spectrum at every temperature as shown in Fig. 4 for $T=300$ K, where we have also reported the fit for the phonon part of the 90° depolarized spectrum. The fit to the experimental data cannot be distinguished from those performed in Sec. IV A. Furthermore, as seen in Figs. 5–7, they yield relaxation times, infinite shear moduli, and thus viscosities quite similar to those of the first fit: the values of the shear modulus are not sensitive to the choice of $R(\omega)$.

C. High-frequency part of the frequency-dependent viscosity

In the two preceding fits, which used the same form for $\eta_S(\omega)$, the experimental static shear viscosity was never retrieved. This can be traced back to our inability to separate, in the line shape of the transverse phonon spectra, the contribution of the shear relaxation time τ_s from the other contributions [terms in g_s and γ_s in Eq. (10)]. To explore the possible role of the critical decay defined by Götze and Sjögren [2] on this line shape, and on the value of τ_s, we have ignored, for this study, the role of the fast relaxation process ($\gamma_s=0$). Furthermore, in order to keep the number of fit parameters as small as possible, we have fixed the value of the parameter a in Eq. (10) to $a=0.33$, a value taken from a previous study of depolarized light scattering [6] in supercooled OTP. We introduce also a constraint between τ_s and τ_R. Taking the shear relaxation time τ_s equal to the rotational time τ_R does not change appreciably the shear modulus but the viscosity obtained from Eq. (11) is constantly higher than the experimental one, a result that is not possible. Then we have taken shear relaxation times proportional to rotational times and tried several ratios $\tau_R/\tau_s=\lambda$ ($\lambda=20$, 10, 5, and 3). At each temperature, fits of nearly equal quality were obtained, whatever λ, while the value of G_∞^α was nearly independent of the value of that parameter: this last result is in line with our earlier remark that, as $r\sim 1$, G_∞^α is basically fixed by the position of the phonon peak in the 90° depolarized spectra. The best agreement with direct experimental values of the shear viscosity was obtained for the ratio $\tau_R/\tau_s\sim 10$. This ratio is constant over the whole temperature range, as seen in Fig. 5, which means that there is no important decoupling between the two corresponding relaxation times in this range. We shall assume that this result remains valid in the pressure domain we shall explore in the following section, i.e., the value of λ is not depending on pressure in the explored domain.

V. ANALYSIS AT HIGH PRESSURE

In this section, we shall first propose an approximation for the variation of the α relaxation time with temperature and pressure, using several light scattering experiments performed in OTP. Then these curves will be used in order to analyze the variation of the transverse Brillouin lines observed at variable pressure and temperature. From this analysis, one can extract the static shear viscosity. Comparing with experimental viscosities already published, we shall consider the description of the temperature-pressure variation of the relaxation times and discuss the respective importance of the temperature and density contributions to the variation of the relaxation time.

A. Pressure and thermal dependence of the α relaxation time

Let us first consider in Fig. 8 the experimental data giving the light scattering α relaxation times [6] at ambient pressure. These values result from the association of several light scattering techniques and cover a very large range of time. A Vogel-Fulcher approximation to these orientational relaxation times is given in the same figure. This approximation is reasonable within a factor of 2 in the range 260–355 K. It overestimates the relaxation time below 260 K and underestimates it above 355 K [38].

Several experiments have been performed on OTP at variable temperature and pressure: Atake and Angell [9] showed that the pressure variation of the glass transition temperature, $dT_g/dP=0.26$ K/MPa, is one of the largest observed in molecular liquids. Other experiments yield the variation of the α relaxation times: dielectric absorption [11], specific heat spectroscopy [14], and photon correlation spectroscopy [12]. In the latter, the same orientational time as in Ref. [6] is measured, but in a limited thermal range. In all these experiments, relaxation times ranging from 0.1 s down to about 10^{-5} s were measured. In the three papers, fits to the experimental data were proposed by means of an extension of the

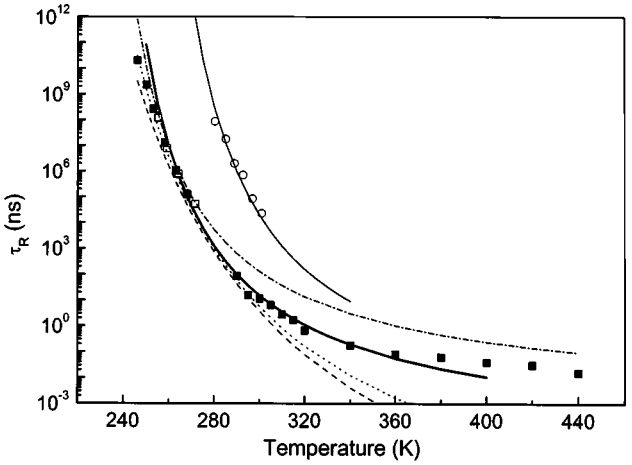

FIG. 8. Rotational relaxation time. Experimental values from Ref. [12], (□) ambient pressure, (○) 100 MPa; experimental values from Ref. [6], ambient pressure, (■); (— — —) Naoki approximation [11]; (· · · · · · · · ·) Leyser approximation [14]; (— — —) Fytas approximation [12]. Interpolation formula, Eq. (14), with numerical values of Table I: 0.1 MPa (——); 100 MPa (——).

Vogel-Fulcher law under the form

$$\tau = \tau_0 \exp\left[\frac{B+\alpha P}{T-(T_0+bP)}\right]. \qquad (13)$$

Unfortunately, the values of the different parameters (b, a, T_0, and τ_0) differ, as seen in Table I, and we have to decide whether there exists a set of parameters which could be used in the analysis of our own data.

The values predicted by the interpolation formulas in Refs. [11], [12], [14] are shown in Fig. 8(a) together with the complete series of relaxation times obtained at ambient pressure [6]. Note that the three high-pressure experiments were performed in a temperature range that only partly coincides with the temperature range of Ref. [6]. Extrapolated to the thermal range which we are interested in, none of the three formulas agrees with the experimental data of Ref. [6]. Therefore to evaluate the pressure variation of orientational relaxation in the range of interest, we have first revisited the extrapolation of the data. The method used here is the following: b, the shift of T_0 with pressure, is taken from Ref. [12]. As seen in Table I, this shift is also very close to the value given in Ref. [11]. Then the ratio $(B+\alpha P)/(T_0+bP)=D$ was taken to be independent of P, optimizing simultaneously the thermal variation of the relaxation time at 0.1 and 100 MPa given in Ref. [12], thus allowing to fix B and α. To compensate for the pressure variation of τ, the parameter $\tau_0(P)$ was here allowed to vary with pressure and its value was approximated by a quadratic function of pressure. The final result is reported in Table I. Values of τ obtained from the interpolation formula are given in Fig. 8 for 0.1 and 100 MPa.

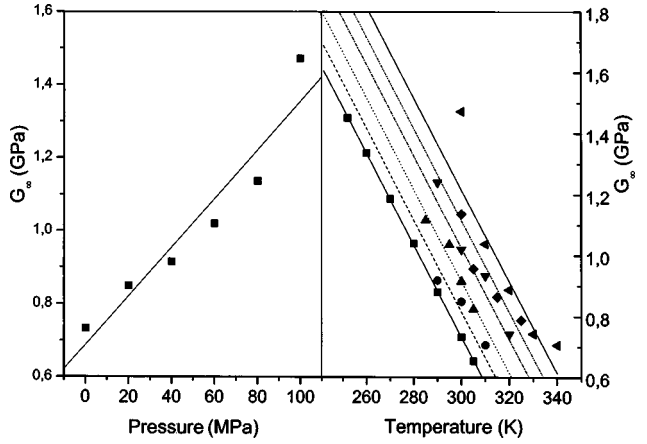

FIG. 9. Temperature and pressure variations of the infinite frequency shear modulus G_∞^α: (a) Pressure variation at 300 K. (b) Temperature variation: (■) 0.1, (●) 20, (▲) 40, (▼) 60, (♦) 80, (◀) 100 MPa; lines, interpolation formula, Eq. (15).

The stretching parameter β is supposed to vary with the pressure. The approximation formula taken to describe the temperature-pressure variation of β [11,6] is purely phenomenological:

$$\beta = 1.09 - 0.6 \exp[-0.022(T-(252+0.2P)] \qquad (14)$$

with T in kelvin and P in megapascal.

Another temperature-independent value $\beta=0.8$ has also been published [7]. In the range of interest, the consequences of this discrepancy on the results reported below are minimal.

B. Analysis of the transverse Brillouin lines

In the fit of the transverse Brillouin lines, the ratio τ_R/τ_s is kept constant ($\tau_R/\tau_s=10$). Examples of the experimental spectra and fits are given in Figs. 3 and 4, respectively, at constant temperature and variable pressure and at constant pressure and variable temperature. In Figs. 9(a) and 9(b), the pressure variation of the infinite frequency shear modulus at room temperature and variable pressure, and at variable temperature and variable pressure, are shown. Together with the

TABLE I. Parameters of Eq. (14). In Eq. (14), $\tau_0(P)=\tau_0+\tau_1 P+\tau_2 P^2$.

Ref.	T_0 (K)	b (K MPa^{-1})	B (K)	α (K MPa^{-1})	τ_0 (s)	τ_1 (s MPa^{-1})	τ_2 (s MPa^{-2})
[12]	219	0.2	921	0.56	1.5×10^{-12}	0	0
[11]	170	0.19	3779	3.43	8.9×10^{-22}	0	0
[14]	191	0.29	2500	0.3	8.9×10^{-19}	0	0
This work	221	0.2	1027	0.932	3.25×10^{-14}	3.17×10^{-16}	4.21×10^{-18}

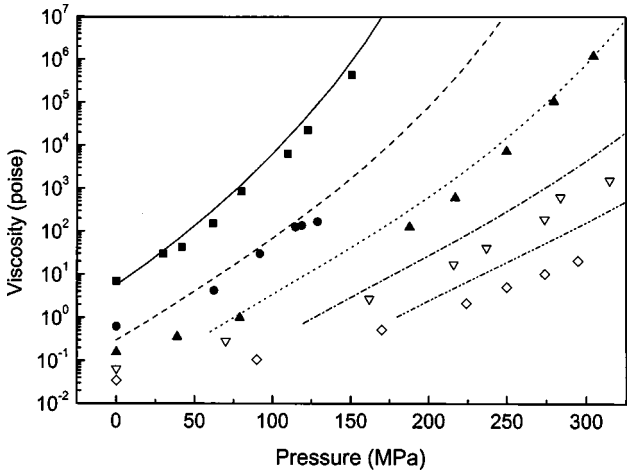

FIG. 10. Static shear viscosity η_S: comparison between $\eta_S = 0.1\tau_R \beta G_\infty^\alpha$ [τ_R, β, and G_∞^α obtained from Eqs. (14)–(16)] and direct measurements [15]. (■) 303, (●) 323, (▲) 343 K; (▽) 363 K; (◇) 383 K.

experimental points, a linear approximation of the temperature and pressure variation of the shear modulus is also given:

$$G_\infty(T,P) = 5.247\times 10^9 + 5\times 10^6 P - 1.505\times 10^7 T \quad (15)$$

with P in megapascal and T in kelvin.

From the values of τ_S, G_∞, and β, viscosities can be computed. In Fig. 10, the values of the static shear viscosity measured by Shug, King, and Böhmer [15] are compared with our analytical estimate for the viscosity. For the three temperatures and pressures up to 300 MPa, the agreement between our estimate and the experimental values is strikingly good. Let us notice that this includes temperature-pressure regions where no Brillouin measurements were carried out. Although at higher temperatures also studied by Shug, King, and Böhmer deviations are observed, our results validate the interpolation scheme proposed for the rotational relaxation time over a large range of pressure and temperature.

C. Density versus temperature contribution to the relaxation

Most results in the literature give the variation of the relaxation time as a function of temperature and pressure. In order to separate between the effects of density and the temperature effects, it is worthwhile [1] to express the relaxation times as a function of temperature and density. From Eq. (14), Table I of this work and Eq. (1), Table I of Ref. [10], we have extracted [39] the variation of the relaxation time versus temperature T at constant density and versus density ρ at constant temperature in the region 250–340 K, 0.1–80 MPa. The variations are shown in Figs. 11(a) and 11(b). At the lowest temperatures [Fig. 11(a)], the variation of the relaxation time along the isotherms with the density is much steeper in the case of OTP than what has been previously observed in glycerol [1]. Tölle *et al.* [13] deduced from an MCT analysis of inelastic incoherent neutron scattering experiments at four temperatures and variable pressure up to

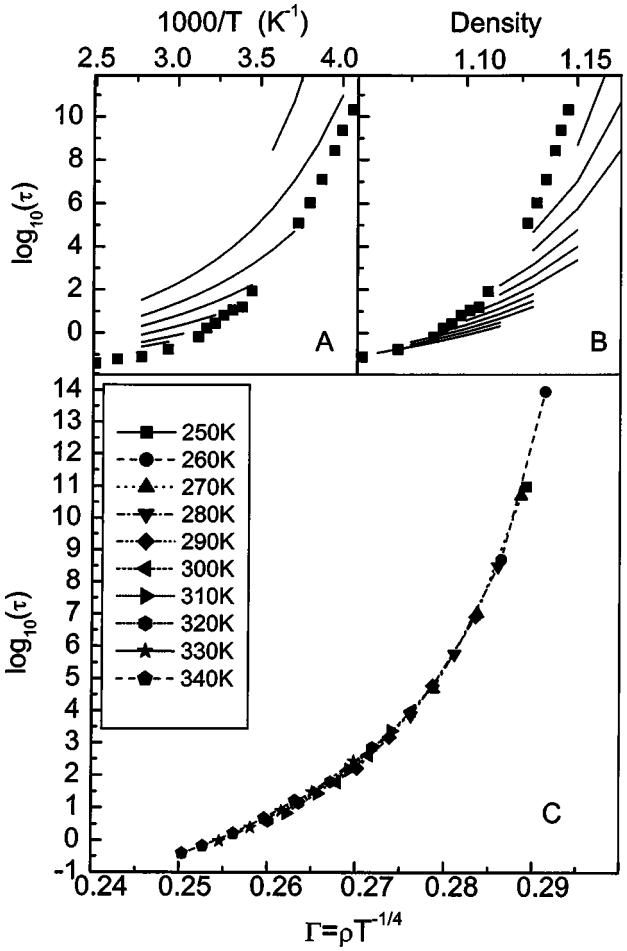

FIG. 11. (a) Thermal variation of the rotational relaxation time at different densities: from bottom to top, $\rho = 1.075$, 1.085, 1.1, 1.115, 1.13, 1.15, and 1.17. (b) Density variation of the rotational relaxation time at different temperatures: from bottom to top, $T = 260$, 270, 280, 290, 300, 310, 320, 330, 340, 350, and 360 K. (c) Variation of the rotational relaxation time τ_R with $\rho T^{-1/4}$ plotted at variable pressure for different temperatures. Lines are obtained from the interpolation formulas.

180 MPa that OTP behaves as a soft sphere system with a repulsive potential in r^{-12}. Such an hypothesis leads [44] to a description of the supercooled liquids in term of a single control parameter $\Gamma = \rho T^{-1/4}$. Our interpolation formula with coefficients given in Table I agree with the Tölle result: we show that indeed $\tau(\rho,T)$ can be plotted as a function of this unique parameter, $\tau(\rho,T) = \tau(\Gamma)$. This could be attributed to the fact that the intermolecular potential between the OTP molecules is mostly dominated by van der Waals interactions. Under pressure, the part of the potential governing the equilibrium properties is mainly the soft core part in r^{-12}.

From the results reported above, we can also attempt to separate temperature and density effects along an isobar. A pertinent parameter allowing this discussion has been defined by Ferrer *et al.* [1]. Together with the usual coefficient of isobaric expansivity α_P, they define a coefficient of isochronic expansivity $\alpha_\tau = -(1/\rho)(\partial\rho/\partial T)_\tau$ (i.e., expansivity at

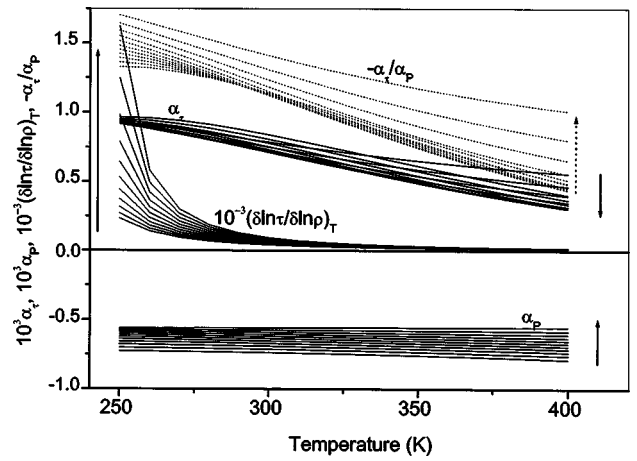

FIG. 12. Thermal variation of $10^3\alpha_\tau$, $10^3\alpha_P$, $10^{-3}(\partial \ln \tau/\partial \ln \rho)_T$, and of the ratio $|\alpha_\tau/\alpha_P|$, at constant pressures ($P=0.1$, 10, 20, 30, 40, 50, 60, 70, 80, 90, and 100 MPa, P increasing following the arrows).

constant relaxation time τ), and write the relaxation time as a function of these coefficients:

$$\ln\left(\frac{\tau(T_g)}{\tau(T)}\right)_{P=\text{const}} = -\int_{(T)}^{(T_g)} dT \left(\frac{\partial \ln \tau}{\partial \ln \rho}\right)_T (-\alpha_\tau + \alpha_P). \tag{16}$$

In Fig. 12, the different contributions to the integrand are shown. The first factor $(\partial \ln \tau/\partial \ln \rho)_T$ varies much more rapidly than the two terms in the second one, so that Eq. (16) can be approximated by

$$\ln\left(\frac{\tau(T_g)}{\tau(T)}\right) \approx -\overline{(-\alpha_\tau + \alpha_P)} \int_{(T)}^{(T_g)} dT \left(\frac{\partial \ln \tau}{\partial \ln \rho}\right)_T, \tag{17}$$

where $\overline{(-\alpha_\tau+\alpha_P)}$ is the mean value over the thermal range.

The ratio $|\alpha_\tau|/\alpha_P$ between both coefficients measures the relative contributions of the change of temperature at constant density and the change of density at constant temperature to the change of the relaxation time. When $|\alpha_\tau|/\alpha_P > 1$, temperature contributions are larger than density contributions. In the case of glycerol [1], this ratio was found to vary from 17 to 24 for relaxation times varying from 1 to 1000 s and estimates of the ratio performed for several glass formers in the neighborhood of T_g gave similar results although with smaller values.

After some algebra, the ratio α_τ/α_P can be expressed as

$$\frac{\alpha_\tau}{\alpha_P} = 1 - \frac{\left(\frac{\partial \rho}{\partial P}\right)_T \left(\frac{\partial \ln \tau}{\partial T}\right)_P}{\left(\frac{\partial \rho}{\partial T}\right)_P \left(\frac{\partial \ln \tau}{\partial P}\right)_T}, \tag{18}$$

so that it can be easily computed from Eq. (13), Table I of this work and Eq. (1), Table I of Ref. [10].

The thermal variation of $|\alpha_\tau/\alpha_P|$ is shown in Fig. 12. We see that down to 314 K, density contributions are dominant. In the range where the approximation to the function $\tau = f(T,P)$ appears reasonable, density effects still contribute about 40% to the viscosity [46].

VI. CONCLUSION

In the present paper, we have studied the transverse propagative Brillouin modes under variable temperature and pressure. From a first analysis of the transverse modes at ambient pressure, built on a single α relaxation process for the shear relaxation, we have extracted the shear relaxation time and the infinite frequency shear modulus. The shear relaxation times were found to be much smaller than the orientational ones and to be too small with respect to the value anticipated for shear viscosity measurements. The fact that shear relaxation time is too small is presumably related to a higher-frequency relaxation part in the relaxation function. Adding a power law to represent it allows us to recover the experimental shear viscosity provided that the shear relaxation time is approximately one-tenth of the rotational one. Turning to experiments at higher pressure and keeping the same one-tenth ratio between the shear and the rotational relaxation times, we found very good agreement with direct viscosity measurements performed under pressure. This allows us to validate the pressure-temperature dependence of the rotational relaxation time that we have deduced from the comparison between different measurements of structural relaxation times at variable temperature and pressure. With the help of the known equation of state for OTP [10], we find that rotational relaxation times are only a function of $\Gamma = \rho T^{-1/4}$, a behavior which could be linked with the pure Lennard-Jones characteristics of the intermolecular potential of OTP. Extension to other glass-forming liquids is required in order to check the degree of generality of the present result. Following the method of Ferrer *et al.*, we have also deduced from those results the temperature and density contributions to the variation of the relaxation time along an isobar. We found that the temperature contribution is larger than the density one at low temperature, while it is the contrary at higher temperature. However, both contributions are always of the same order of magnitude in the whole range of temperature and pressure explored.

ACKNOWLEDGMENTS

We gratefully acknowledge Thomas Franosch and Herman Z. Cummins for useful discussions and comments. C.D. and W.S. benefited by a CNRS/Max-Planck Gesellschaft agreement between PMC (UMR 7602-CNRS and Université Pierre et Marie Curie) and Max Planck Institute for Polymer Research in Mainz.

APPENDIX

Equation (10) represents a form of $\omega\eta_S(\omega)$ appropriate to the range of frequency ($\approx$1–10 GHz) necessary to analyze the 90° depolarized spectra. Nevertheless, Eq. (11) makes use of the $\omega \to 0$ limit of $\eta_S(\omega)$ which diverges [see Eq. (10)] because the coefficient characterizing the critical decay is smaller than unity.

This result is simply a mathematical artifact linked to the approximation used when writing Eq. (10). The critical decay is the first step of the fast relaxation process and is represented in the time domain by a power law, t^{-a}. This decay takes place for times much shorter than the α relaxation time, τ_s. Conversely, the α relaxation process is characterized by a stretched exponential decay, $\exp[-(t/\tau_s)^{\beta}]$ with $\beta<1$. The wrong $\omega\rightarrow 0$ limit of ω^{a-1} is related to the too slow decay of the t^{-a} function for $t\geqslant\tau_s$, which is an incorrect representation of $\eta_S(t)$ for longer times. This can be remedied by expressing [45] the critical decay as $\eta_{S,\mathrm{crit}}(t) \approx t^{-a}\exp(-t/\tau_s)$: $\eta_{S,\mathrm{crit}}(t)$ has the correct analytical form in the region where $\eta_S(t)$ is the critical decay and decays to zero much faster than the stretched exponential when the latter dominates. The Laplace transform of $\eta_{S,\mathrm{crit}}(t)$ is easily found [45] to be proportional to

$$i\left(\omega-\frac{i}{\tau_s}\right)^{a-1} \tag{A1}$$

and one can check that this expression is consistent with our use of Eq. (10). Indeed, the shortest values of τ_s used in the present study are of the order of the nanosecond, so that the product $\omega_B\tau_s$ (where ω_B is the peak of the phonon part of the depolarized 90° spectrum) is always much larger than unity. This means that

$$\omega\,\eta_{S,\mathrm{crit}}(\omega)\approx\omega\left(\omega-\frac{i}{\tau_s}\right)^{a-1}\approx\omega^{a} \tag{A2}$$

in the region we used it. The correct expression for $\eta_S(\omega)$ to be used in the $\omega\rightarrow 0$ limit is thus

$$\eta_S(\omega)\approx\frac{1}{\omega}G_{\infty}^{\alpha}\left[1-\left(\frac{1}{1+i\omega\tau_s}\right)^{\beta_L}\right] +i\left[\left(\frac{i}{\tau_s}+\omega\right)^{a-1}g_s+\gamma_s\right]^{a}. \tag{A3}$$

with $a=0.33$. This yields

$$\eta_S=\beta_L G_{\infty}^{\alpha}\tau_s+\tau_s^{1-a}g_s\cos\pi a/2+\gamma_s. \tag{A3a}$$

In our experiment, at 300 K and 0.1 MPa, $\gamma_s\approx 10^{-2}$ P and $g_s\tau_s^{1-a}\approx 1$ P while $\eta_S\approx 10$ P. Neglecting γ_s and g_s in Eq. (11) is thus perfectly legitimate at 300 K; furthermore, the ratio $g_s\tau_s^{1-a}/\eta_S\propto\tau_s^{-a}$ will decrease with decreasing temperature.

Let us now turn to the $\omega\rightarrow\infty$ limit, i.e., to the contribution of the fast relaxation processes to the sound velocity when the transverse modes become propagative. In the vicinity of the Brillouin peak, the frequency dependence of the imaginary part of $\omega\eta_S(\omega)$ may be written as

$$\omega A\equiv\omega[a\,\omega_B^{a-1}g_s+\gamma_s]. \tag{A4}$$

This means that, in the vicinity of the Brillouin peak, the denominator of the second term of Eq. (6) may be written as

$$\left(\omega-i\frac{q^2A}{2\rho_m}\right)^2-\frac{q^2}{\rho_m}\left(G_{\infty}^{\alpha}-\frac{q^2A^2}{4\rho_m}\right). \tag{A5}$$

In our depolarized 90° experiments, the Brillouin peak is located in the vicinity of 4 GHz. A $\omega_B^{a-1}g_s\approx 3\times 10^{-6}$ P is much smaller than γ_s and $q^2A^2/4\rho_m\approx 1.2\times 10^5$ Pa, which is negligible with respect to $G_{\infty}^{\alpha}>5\times 10^8$ Pa. Thus the $\omega\rightarrow\infty$ limit of $\omega\eta_S(\omega)$ can be safely taken as G_{∞}^{α}, as implied in Eq. (12).

[1] M. L. Ferrer, C. Lawrence, B. G. Demirjan, D. Kivelson, C. Alba-Simionesco, and G. Tarjus, J. Chem. Phys. **109**, 8010 (1998).

[2] W. Götze and L. Sjögren, Rep. Prog. Phys. **55**, 241 (1992); W. Götze, in *Liquids Freezing and the Glass Transition*, edited by J. P. Hansen, D. Levesque, and J. Zinn-Justin (North-Holland, Amsterdam, 1990) p. 287.

[3] C. A. Angell, Science **267**, 1924 (1995).

[4] A. Tölle, Rep. Prog. Phys. **64**, 1473 (2001), and references therein.

[5] C. H. Wang, X. R. Zhu, and J. C. Shen, Mol. Phys. **62**, 749 (1987).

[6] (a) W. Steffen, A. Patkowski, H. Gläser, G. Meier, and E. W. Fischer, Phys. Rev. E **49**, 2992 (1994); (b) W. Steffen, B. Zimmer, A. Patkowski, G. Meier, and E. W. Fischer, J. Non-Cryst. Solids **172-174**, 37 (1994).

[7] H. Z. Cummins, Y. H. Wang, Gen Li, W. M. Du, W. Osert, and G. Q. Shen, J. Non-Cryst. Solids **235**, 254 (1998).

[8] (a) G. Monaco, D. Fioretto, L. Comez, and G. Ruocco, Phys. Rev. E **63**, 061502 (2002); G. Monaco, S. Caponi, R. di Leonardo, D. Fioretto, and G. Ruocco, *ibid.* **62**, R7595 (2000); (b) G. Monaco, D. Fioretto, C. Masciovecchio, G. Ruocco, and F. Sette, Phys. Rev. Lett. **82**, 1776 (1999).

[9] T. Atake and C. A. Angell, J. Phys. Chem. **83**, 3218 (1979).

[10] M. Naoki and S. Koeda, J. Phys. Chem. **93**, 948 (1989).

[11] M. Naoki, H. Endou, and K. Matsumoto, J. Phys. Chem. **91**, 4169 (1987).

[12] G. Fytas, Th. Dorfmuller, and C. H. Wang, J. Phys. Chem. **87**, 5041 (1983).

[13] A. Tölle, H. Schober, J. Wuttke, O. G. Randl, and F. Fujura, Phys. Rev. Lett. **80**, 2374 (1998).

[14] H. Leyser, A. Schulte, W. Doster, and W. Petry, Phys. Rev. E **51**, 5899 (1995).

[15] K. U. Shug, H. E. King, Jr., and R. Böhmer, J. Chem. Phys. **109**, 1472 (1998).

[16] J. P. Hansen and I. R. McDonald, *Theory of Simple Liquids*,

2nd ed. (Academic, London, 1990).
[17] G. D. Enright and B. P. Stoicheff, J. Chem. Phys. **64**, 3658 (1976).
[18] H. C. Andersen and R. Pecora, J. Chem. Phys. **54**, 2584 (1971); **55**, 1496 (1971); P. J. Chapell, M. P. Allen, P. I. Hallen, and D. Kivelson, *ibid.* **74**, 5929 (1981).
[19] B. Quentrec, Phys. Rev. A **15**, 1304 (1977).
[20] C. H. Wang, Mol. Phys. **58**, 497 (1986).
[21] C. Dreyfus, A. Aouadi, R. M. Pick, T. Berger, A. Patkowski, and W. Steffen, Europhys. Lett. **42**, 55 (1998); C. Dreyfus, A. Aouadi, R. M. Pick, T. Berger, A. Patkowski, and W. Steffen, Eur. Phys. J. B **9**, 401 (1999).
[22] T. Franosch, A. Latz, and R. M. Pick, Eur. Phys. J. B **31**, 229 (2003).
[23] C. Dreyfus, M. J. Lebon, F. Vivicorsi, A. Aouadi, R. M. Pick, and H. Z. Cummins, Phys. Rev. E **63**, 041509 (2001).
[24] B. Berne and R. Pecora, *Dynamic Light Scattering* (Wiley, New York, 1976).
[25] The Fourier transform is given here by $f(\omega) = i\int_0^\infty e^{-i\omega t} f(t)dt$.
[26] C. P. Lindsey and G. D. Patterson, J. Chem. Phys. **73**, 3348 (1980).
[27] G. Li, W. M. Du, X. K. Chen, H. Z. Cummins, and N. J. Tao, Phys. Rev. A **45**, 3867 (1992); G. Li, W. M. Du, A. Sakai, and H. Z. Cummins, *ibid.* **46**, 3343 (1992); J. Wüttke, M. Ohl, M. Goldhammer, S. Roth, O. Schneider, P. Leukenheimer, R. Kahn, B. Rufflé, R. Lechner, and M. A. Berg, Phys. Rev. E **61**, 2730 (2000); M. Goldammer, C. Losert, J. Wuttke, W. Petry, F. Terki, H. Schober, and P. Lunkenheimer, *ibid.* **64**, 021303 (2001).
[28] W. M. Du, G. Li, H. Z. Cummins, M. Fuchs, J. Toulouse, and L. A. Knauss, Phys. Rev. E **49**, 2192 (1994). In this paper, the critical part is represented by a complex function while we have used a pure imaginary function. This results in a shift in the shear modulus which is neglected in our description. However, as shown in the Appendix, this shift is negligible in OTP.
[29] W. Steffen, A. Patkowski, H. Glaeser, G. Meier, and E. W. Fischer, Phys. Rev. E **49**, 2992 (1994).
[30] J. Gapinski, W. Steffen, A. Patkowski, A. P. Sokolov, A. Kisliuk, U. Buchenau, M. Russina, F. Mezei, and H. Schober, J. Chem. Phys. **110**, 2312 (1999).
[31] G. Fytas, A. Patkowski, G. Meier, and T. H. Dorfmüller, Macromolecules **15**, 214 (1982); J. Chem. Phys. **80**, 2214 (1984).
[32] Note that thermal variation of β_{CD} is varying from 0.55 to 0.90 in the temperature range used here [6,7].
[33] Another estimate was made from Ref. [8(b)], assuming the instantaneous linewidth contribution to the longitudinal and transverse linewidths to be the same. Both values are small compared to the widths of the transverse modes, so that their difference makes no appreciable change in the parameters obtained in the fit.
[34] R. M. Pick *et al.* (unpublished).
[35] R. Torre, A. Taschin, and M. Sampoli, Phys. Rev. E **64**, 061504 (2001).
[36] C. Glorieux, K. A. Nelson, G. Hinze, and M. D. Fayer, J. Chem. Phys. **116**, 3384 (2002).
[37] A. Taschin, R. Torre, M. Ricci, M. Sampoli, C. Dreyfus, and R. M. Pick, Europhys. Lett. **56**, 407 (2001).
[38] Deviations to the VFT approximation to the activation plot have been extensively studied in C. Hansen, F. Stickel, T. Berger, R. Richert, and E. W. Fischer, J. Chem. Phys. **107**, 1086 (1997). Other approximations to the activation plot than a simple Vogel-Fulcher function can be found is this paper and in Ref. [28].
[39] S. Haykin, *Neural Networks: A Comprehensive Foundation* (Macmillan, New York, 1994).
[40] E. McLaughlin and A. R. Ubbelohe, Trans. Faraday Soc. **54**, 1804 (1957).
[41] R. J. Greet and D. Turnbull, J. Chem. Phys. **46**, 1243 (1967).
[42] W. T. Laughlin and D. R. Uhlmann, J. Phys. Chem. **76**, 2317 (1972).
[43] W. T. Cukierman, M. Lane, and D. R. Uhlmann, J. Chem. Phys. **59**, 3639 (1973).
[44] J. P. Hansen and I. R. McDonald, in *Theory of Simple Liquids* (Ref. [16]), p. 155.
[45] A. Brodin, M. Frank, S. Wiebel, G. Q. Shen, J. Wuttke, and H. Z. Cummins, Phys. Rev. E **65**, 051503 (2002).
[46] Other values of the ratio α_τ/α_P have been recently published for two glass forming liquids in M. Paluch, C. M. Roland, R. Casalini, G. Meier, and A. Patkowski, J. Chem. Phys. **118**, 4578 (2003).